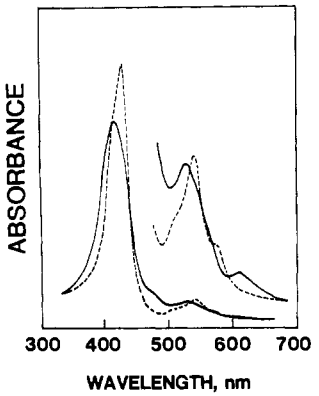

Figure 10. Time-resolved thin-layer spectra after controlled-potential electrolysis of (TMP)Fe(NO) at 0.76 V in CH_2Cl_2 containing 0.1 M TBAP and 4.0×10^{-2} M pyridine: (—) initial spectrum; (---) final spectrum.

UV-visible spectral changes during time-resolved oxidation of (TMP)Fe(NO) at 0.76 V in CH_2Cl_2, 0.1 M TBAP containing 4.0×10^{-2} M pyridine are shown in Figure 10. There are no well-defined isosbestic points, indicating that a mixture of $[(TMP)Fe(NO)(py)]^+$ and $[(TMP)Fe(py)_2]^+$ is produced. This is in agreement with the FTIR spectral data, as well as other UV-visible data in the literature for (TPP)Fe(NO) in pyridine or mixed-solvent systems containing pyridine,[11] which shows that longer electrolysis times lead to higher concentrations of $[(P)Fe(py)_2]^+$ in solution. This reaction is given by eq 5.

The final UV-visible spectrum after electrooxidation of (TMP)Fe(NO) in the presence of pyridine has a Soret band at 428 nm, visible bands at 543 and 576 nm, and a shoulder at 512 nm. This spectrum is similar to those of both six-coordinate (TPP)Fe(NO)Cl[7] and six-coordinate $(TPP)Fe(L)_2(Cl)$,[36] thus suggesting that a mixture of $[(TMP)Fe(NO)(py)]^+$ and $[(TMP)Fe(py)_2]^+$ is most likely present in solution.

In conclusion, the techniques of FTIR and UV-visible thin-layer spectroelectrochemistry can be utilized to monitor the site of electrooxidation, the fate of the bound NO group after electrooxidation, the linearity of the Fe-N-O bond in the electrooxidized product, and the presence of a coordinated neutral or ionic trans axial ligand in electrooxidized iron nitrosyl porphyrins. The IR bands for NO are well defined in (P)Fe(NO), $[(P)Fe(NO)]^+$, (P)Fe(NO)X, and $[(P)Fe(NO)(S)]^+$ complexes, and the specific frequencies, which vary from 1667 to 1925 cm^{-1}, clearly indicate the iron oxidation state, the linearity of the Fe-N-O bond, and the coordination number of the central iron atom.

Acknowledgment. The support of the National Institutes of Health (Grant GM 25172) is gratefully acknowledged.

Registry No. TBAP, 1923-70-2; (TMP)Fe(NO), 117470-05-0; $(TMP)Fe(NO)^+$, 117470-06-1; $(TMP)Fe(NO)^{2+}$, 117470-07-2; $(TMP)Fe(NO)^{3+}$, 117470-10-7; (TPP)Fe(NO), 52674-29-0; $(TPP)Fe(NO)^+$, 70622-46-7; $(TPP)Fe(NO)^{2+}$, 117470-08-3; $(TPP)Fe(NO)^{3+}$, 117470-11-8; (OEP)Fe(NO), 55917-58-3; $(OEP)Fe(NO)^+$, 89596-92-9; $(OEP)Fe(NO)^{2+}$, 117470-09-4; $(OEP)Fe(NO)^{3+}$, 117470-12-9; (TPP)Fe(NO)I, 117470-13-0; (TMP)Fe(NO)I, 117470-15-2; (OEP)Fe(NO)I, 117470-18-5; (TPP)Fe(NO)Br, 117470-14-1; (TMP)Fe(NO)Br, 117470-16-3; (OEP)Fe(NO)Br, 117470-19-6; (TPP)Fe(NO)Cl, 50262-98-1; (TMP)Fe(NO)Cl, 117470-17-4; (OEP)Fe(NO)Cl, 117470-20-9; $[(TPP)Fe(NO)(DMSO)]^+$, 117470-21-0; $[(TMP)Fe(NO)(DMSO)]^+$, 117470-27-6; $[(OEP)Fe(NO)(DMSO)]^+$, 117470-33-4; $[(TPP)Fe(NO)(DMA)]^+$, 117470-22-1; $[(TMP)Fe(NO)(DMA)]^+$, 117470-28-7; $[(OEP)Fe(NO)(DMA)]^+$, 117470-34-5; $[(TPP)Fe(NO)(THF)]^+$, 117470-23-2; $[(TMP)Fe(NO)(THF)]^+$, 117470-29-8; $[(OEP)Fe(NO)(THF)]^+$, 117470-35-6; $[(TPP)Fe(NO)(DMF)]^+$, 117470-24-3; $[(TMP)Fe(NO)(DMF)]^+$, 117470-30-1; $[(OEP)Fe(NO)(DMF)]^+$, 117470-36-7; $[(TPP)Fe(NO)(py)]^+$, 117470-25-4; $[(TMP)Fe(NO)(py)]^+$, 117470-31-2; $[(OEP)Fe(NO)(py)]^+$, 117470-37-8; $[(TPP)Fe(NO)(PhCN)]^+$, 117470-26-5; $[(TMP)Fe(NO)(PhCN)]^+$, 117470-32-3; $[(OEP)Fe(NO)(PhCN)]^+$, 117470-38-9.

(36) Walker, F. A.; Lo Man-Wai; Ree, M. T. *J. Am. Chem. Soc.* **1976**, *98*, 5552.

Contribution from the Department of Chemistry, University of Notre Dame, Notre Dame, Indiana 46556

Reactions of SO_2 with Iron Porphyrinates and the Crystal Structure of (Hydrogen sulfato)(tetraphenylporphinato)iron(III) Hemibenzene Solvate

W. Robert Scheidt,* Young Ja Lee, and Michael G. Finnegan

Received July 14, 1988

The reactions of $Fe^{II}TPP$ and $Fe^{III}TPP$ with sulfur dioxide have been investigated as part of a study of potential coordination chemistry models for sulfite and nitrite reductase. Although the solubility of $Fe^{II}TPP$ in a variety of solvents is significantly increased by the addition of SO_2 to the solvent, we have been unable to isolate any SO_2 adducts. We do find that the presence of SO_2 substantially increases the oxidation sensitivity of iron(II) porphyrinates. We have isolated three different sulfato complexes of (porphinato)iron(III): the previously reported binuclear species, $[Fe(TPP)]_2SO_4$, a mononuclear bisulfate complex, $[Fe(TPP)(OSO_3H)]$, and a third sulfate-containing derivative. The species have been characterized by UV-vis and IR spectroscopy, and the $[Fe(TPP)(OSO_3H)]$ complex has also been the subject of a single-crystal X-ray structure determination. This investigation revealed a monodentate hydrogen sulfato ligand leading to a five-coordinate high-spin iron(III) complex. The axial Fe-O bond distance is 1.926 Å, and the average Fe-N bond distance is 2.042 Å. Crystal data for $[Fe(TPP)(OSO_3H)]\cdot{}^1/_2C_6H_6$: monoclinic, $a = 16.981$ (5) Å, $b = 13.559$ (3) Å, $c = 33.456$ (5) Å, $\beta = 99.88$ (2)°, $Z = 8$, space group $P2/c$, 5990 unique observed data, $R_1 = 0.052$, $R_2 = 0.059$, all observations at 293 K. The reaction of sulfur trioxide with $[Fe(TPP)]_2O$ has also been briefly investigated: $[Fe(TPP)]_2SO_4$ is produced.

Sulfite reductase is a plant and bacterial enzymatic system that carries out the reduction of sulfite ion to hydrogen sulfide.[1] This unusual enzyme is one of three known systems carrying out a six-electron reduction reaction; the others are nitrogenase and nitrite reductase. It is apparently closely related to assimilatory nitrite reductases in terms of prosthetic group[2] (siroheme[3,4] and a closely coupled Fe-S cluster[5]) and probably in terms of catalytic pathway (a series of two-electron steps has been postulated). Both

(1) Siegel, L. M.; Davis, P. S.; Kamin, H. *J. Biol. Chem.* **1974**, *249*, 1572. Siegel, L. M. In *Metabolism of Sulfur Compounds*; Greenberg, D. M., Ed.; Academic: New York, 1975; pp 217-286.

(2) Krueger, R. J.; Seigel, L. M. *Biochemistry* **1982**, *21*, 2892-2904.

(3) Siroheme is a tetrahydroporphyrin derivative. However, in view of the known reaction similarity of porphyrins and tetrahydroporphyrins,[4] all of our studies have utilized the more accessible porphyrin species as the target complex.

(4) Stolzenberg, A. M.; Strauss, S. H.; Holm, R. H. *J. Am. Chem. Soc.* **1981**, *103*, 4763-4778. Fujita, E.; Chang, C. K.; Fajer, J. *J. Am. Chem. Soc.* **1985**, *107*, 7665-7669.

0020-1669/88/1327-4725$01.50/0

Scheme I

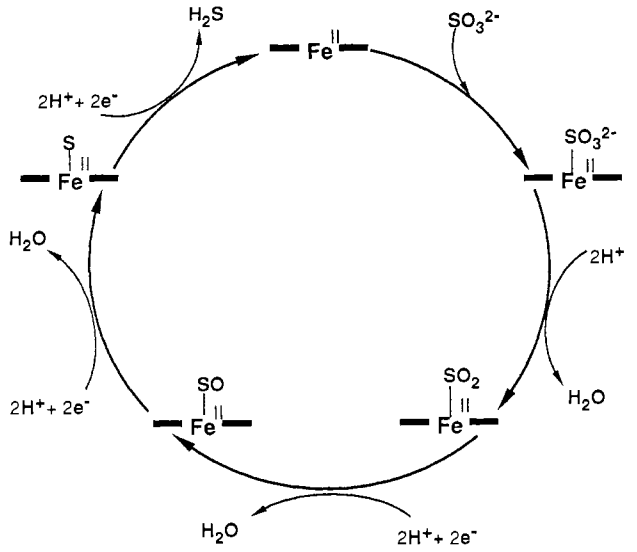

of these related enzymatic systems carry out their reductions rapidly, and no intermediates have yet been definitely observed. By analogy to suggested steps of nitrite reductase, a catalytic cycle for sulfite reductase might involve the steps shown in Scheme I. Only one complex, the sulfide, which is possibly related to species at the end of the cycle, has thus far been reported[6] as an iron porphyrinate species.

We report the results of our attempts to prepare iron porphyrinate complexes related to the presumed early intermediates in the catalytic cycle of sulfite reductase. Our first experiments utilized $Fe^{II}TPP$ (TPP, dianion of tetraphenylporphyrin) and sulfur dioxide; the initial results also led us to briefly examine the interaction of SO_2 with iron(III) porphyrinates. We find no evidence for simple direct reaction of SO_2 and either iron(II) or iron(III) porphyrin derivatives; in all cases only starting materials or products attributable to side reactions involving impurities were observed. We report these reactions herein and present the crystal structure determination of one product, that of the hydrogen sulfate complex of $Fe^{III}TPP$, a previously unisolated substance.

Experimental Section

Methylene chlorine was dried by distillation from CaH_2. Other solvents were dried by distillation from sodium benzophenone ketyl under argon. SO_2 was purchased from Linde Specialty Gases and dried by passing through a column of P_4O_{10} (Aquasorb, Mallinckrodt). All procedures were carried out in Schlenk-type vessels under argon. $Fe^{II}TPP$ was prepared by reduction of solutions of [Fe(TPP)Cl] by zinc amalgam[7] or chromous acetylacetonate.[8] Chromous acetylacetonate was prepared as described previously.[9] Reactions with gaseous SO_2 were carried out on degassed solutions (argon sparge) of $Fe^{II}TPP$ in various solvents (benzene, toluene, THF, methylene chloride). The concentration of $Fe^{II}TPP$ was in the range 5×10^{-3} to 1×10^{-2} M, and SO_2 was bubbled through the solution by using either gas inlet tubes or 22-gauge syringe needles at rates ranging from 0.1 to 4.0 cm^3/min. Products were isolated by removal of solvent under vacuum or by addition of nonsolvents (hexane, heptane, ethanol). Complete details may be seen elsewhere.[10] Standardized solutions of SO_2 in toluene were prepared by bubbling SO_2 through degassed toluene for 20 min and then allowing the solution to equilibrate overnight. SO_2 concentrations were determined by treatment with standardized iodine and titration with aqueous sodium thiosulfate. Reactions with $Fe^{II}TPP$ were then immediately carried out with these solutions, using SO_2/Fe ratios of 1–3 and reaction periods of 10 min to 4 days. Reactions of $Fe^{II}TPP$ were also carried out in liquid SO_2 at −40 °C.

SO_3 was prepared from fuming sulfuric acid (30% excess SO_3) by heating to 60 °C under a stream of argon. The vapors were passed through a P_4O_{10} column and condensed in a Schlenk flask immersed in an ethylene glycol/liquid nitrogen bath. In reactions of $[Fe(TPP)]_2O$ with SO_3, toluene or tetrahydrofuran solutions were treated with a stream of argon that had been passed over solid sulfur trioxide at room temperature. The changes in the UV–visible spectrum are consistent with the formation of $[Fe(TPP)]_2SO_4$. The infrared spectra of isolated solids are also consistent with the preparation of $[Fe(TPP)]_2SO_4$, but other products are also present. It is likely that the SO_3 also attacks the porphyrin.[11]

UV–vis spectra were taken on a Cary 14 or Varian DMS-100 instrument. IR spectra were measured on Perkin-Elmer Model 521 and 727B spectrometers as KBr pellets.

Crystal Structure Determination. Examination of deep purple crystals that proved to be $[Fe(TPP)(OSO_3H)]\cdot{}^1/_2C_6H_6$ on a CAD4 automated diffractometer established an eight-molecule monoclinic unit cell with the cell parameters listed in Table I. Complete details of crystal data and intensity collection are given in Table SI (supplementary material). Data were corrected for the effects of absorption by the ψ-scan empirical method. The systematic absences are consistent with the space groups Pc and $P2/c$. The structure was solved in the centrosymmetric space group $P2/c$ with the direct-methods program MULTAN78.[12] The two independent molecules were found in the E map and a few difference Fourier maps. Two benzene molecules were found along the 2-fold axis. One of the two benzene molecules was disordered and accordingly was refined by using rigid-group techniques. Most hydrogen atoms were found in difference Fourier maps, including the hydrogen atom of each of the HSO_4^- ions. The HSO_4^- protons were included as found in the difference Fourier synthesis while the remaining hydrogen atom positions were idealized (C–H = 0.95 Å, B(H) = 1.2B(C)). All hydrogen atoms were then included in subsequent cycles of least-squares refinement as fixed contributors. At convergence, the final discrepancy indices were $R_1 = 0.052$ and $R_2 = 0.059$ with an error of fit of 1.25. The final difference Fourier map had its largest peak of 0.37 e/Å^3 near the disordered benzene molecule. Final values of atomic coordinates are given in Table II; final values of anisotropic temperature factors are given in Table SII (supplementary material). Fixed hydrogen atom coordinates are reported in Table SIII (supplementary material).

Table I. Crystallographic Data for $[Fe(TPP)(OSO_3H)]\cdot{}^1/_2C_6H_6$

$FeSO_4N_4C_{47}H_{32}$	fw 804.71
a = 16.981 (5) Å	space group $P2/c$
b = 13.559 (3) Å	T = 293 K
c = 33.456 (5) Å	λ = 0.71073 Å
β = 99.88 (2)°	μ = 0.499 mm^{-1}
V = 7588.8 Å^3	$R(F_o)$ = 0.052
Z = 8	$R_w(F_o)$ = 0.059

Results and Discussion

A number of $\{MSO_2\}^{6\,13}$ species are known,[14] and an analogous $\{FeTPP(SO_2)\}^6$ species would seem to be plausible. This plausibility was enhanced by an initial observation, the fact that the solubility of $Fe^{II}TPP$ is significantly enhanced by the addition of SO_2 to the solvent. For example, a greater than 10-fold increase in the solubility of $Fe^{II}TPP$ in acetonitrile is found when the acetonitrile is 3 M in SO_2. In toluene, the rate of dissolution of $Fe^{II}TPP$ is substantially increased by making the solution 0.3 M

(5) Christner, J. A.; Munck, E.; Janick, P. A.; Siegel, L. M. *J. Biol. Chem.* **1981**, *256*, 2098–2101. Janick, P. A.; Siegel, L. M. *Biochemistry* **1982**, *21*, 3538–3547. McRee, D. E.; Richardson, D. C.; Richardson, J. S.; Siegel, L. M. *J. Biol. Chem.* **1986**, *261*, 10277–10286.
(6) English, D. R.; Hendrickson, D. N.; Suslick, K. S.; Eigenbrot, C. W.; Scheidt, W. R. *J. Am. Chem. Soc.* **1984**, *106*, 7258–7259.
(7) Landrum, J. T.; Hatano, K.; Scheidt, W. R.; Reed, C. A. *J. Am. Chem. Soc.* **1980**, *102*, 6729–6735.
(8) Collman, J. P.; Hoard, J. L.; Kim, N.; Reed, C. A. *J. Am. Chem. Soc.* **1975**, *97*, 2676–2681.
(9) Ocone, L. R.; Block, B. P. *Inorg. Synth.* **1966**, *8*, 125–132.
(10) Finnegan, M. G. Ph.D. Thesis, University of Notre Dame, 1988.
(11) Fleischer, E. B.; Palmer, J. M.; Srivastava, T. S.; Chatterjee, A. *J. Am. Chem. Soc.* **1971**, *93*, 3162–3167.
(12) Programs used in this study included local modifications of Main, Hull, Lessinger, Declerq, and Woolfson's MULTAN78, Jacobson's ALLS, Zalkin's FORDAP, Busing and Levy's ORFFE and ORFLS, and Johnson's ORTEP2. Atomic form factors were from: Cromer, D. T.; Mann, J. B. *Acta Crystallogr., Sect. A* **1968**, *A24*, 321–323. Real and imaginary corrections for anomalous dispersion in the form factors of the iron and sulfur atoms were from: Cromer, D. T.; Liberman, D. J. *J. Chem. Phys.* **1970**, *53*, 1891–1898. Scattering factors for hydrogen were from: Stewart, R. F.; Davidson, E. R.; Simpson, W. T. *Ibid.* **1965**, *42*, 3175–3187. All calculations were performed on a VAX 11/730 computer.
(13) The $\{MSO_2\}^6$ notation is used to denote the number of d electrons on the metal and the π^* electrons on the ligand and was originally used for nitrosyl complexes. Cf.: Enemark, J. H.; Feltham, R. D. *Coord. Chem. Rev.* **1974**, *13*, 339–406.
(14) Ryan, R. R.; Kubas, G. J.; Moody, D. C.; Eller, P. G. *Struct. Bonding (Berlin)* **1981**, *46*, 47–100.

Table II. Fractional Atomic Coordinates for [Fe(TPP)(OSO$_3$H)]·$^1/_2$C$_6$H$_6$[a]

atom	x	y	z	atom	x	y	z
Fe(1)	0.56834 (5)	−0.13870 (6)	0.609246 (26)	C(m8)	0.0245 (3)	0.9246 (4)	0.60164 (18)
Fe(2)	0.06124 (5)	0.67117 (5)	0.612756 (26)	C(1)	0.7674 (4)	−0.1950 (4)	0.52224 (19)
S(1)	0.45390 (12)	0.00363 (14)	0.55121 (6)	C(2)	0.8482 (4)	−0.2155 (5)	0.53221 (20)
S(2)	−0.04291 (12)	0.51877 (13)	0.55426 (6)	C(3)	0.8942 (4)	−0.2241 (5)	0.50185 (24)
O(1)	0.49252 (23)	−0.09287 (27)	0.56380 (12)	C(4)	0.8617 (4)	−0.2144 (5)	0.46249 (23)
O(2)	0.5218 (4)	0.0744 (3)	0.54757 (16)	C(5)	0.7824 (4)	−0.1941 (6)	0.45247 (21)
O(3)	0.4051 (3)	−0.0117 (4)	0.51094 (15)	C(6)	0.7351 (4)	−0.1837 (5)	0.48215 (22)
O(4)	0.4095 (3)	0.0410 (4)	0.58028 (16)	C(7)	0.6977 (4)	0.1834 (4)	0.65154 (19)
O(5)	−0.00773 (24)	0.61786 (26)	0.56570 (12)	C(8)	0.6548 (4)	0.2694 (5)	0.64381 (20)
O(6)	−0.0886 (3)	0.5270 (4)	0.51320 (15)	C(9)	0.6916 (5)	0.3608 (5)	0.65076 (23)
O(7)	0.0263 (3)	0.4491 (3)	0.55287 (16)	C(10)	0.7701 (5)	0.3661 (6)	0.66403 (28)
O(8)	−0.0877 (4)	0.4828 (4)	0.58340 (17)	C(11)	0.8149 (5)	0.2830 (6)	0.67082 (27)
N(1)	0.61337 (27)	−0.2638 (3)	0.58682 (14)	C(12)	0.7789 (4)	0.1906 (5)	0.66509 (25)
N(2)	0.67007 (27)	−0.0678 (3)	0.60140 (14)	C(13)	0.3662 (4)	−0.0876 (4)	0.69501 (22)
N(3)	0.55493 (28)	−0.0336 (3)	0.65190 (14)	C(14)	0.3738 (4)	−0.0958 (5)	0.73625 (24)
N(4)	0.49684 (28)	−0.2301 (3)	0.63533 (14)	C(15)	0.3093 (6)	−0.0935 (6)	0.75602 (25)
N(5)	−0.00979 (27)	0.7714 (3)	0.63516 (14)	C(16)	0.2356 (6)	−0.0851 (6)	0.7341 (3)
N(6)	0.04204 (27)	0.5788 (3)	0.65823 (14)	C(17)	0.2234 (5)	−0.0778 (6)	0.6923 (3)
N(7)	0.16235 (27)	0.5935 (3)	0.61011 (14)	C(18)	0.2898 (5)	−0.0781 (5)	0.67298 (24)
N(8)	0.11186 (27)	0.7883 (3)	0.58794 (14)	C(19)	0.4917 (4)	−0.4942 (4)	0.59767 (22)
C(a1)	0.5857 (4)	−0.3594 (4)	0.58695 (18)	C(20)	0.4650 (4)	−0.5301 (5)	0.55905 (23)
C(a2)	0.6732 (4)	−0.2644 (4)	0.56350 (18)	C(21)	0.4378 (4)	−0.6254 (6)	0.55343 (26)
C(a3)	0.7131 (3)	−0.0917 (4)	0.57116 (18)	C(22)	0.4339 (4)	−0.6861 (5)	0.5860 (3)
C(a4)	0.6908 (3)	0.0292 (4)	0.61216 (18)	C(23)	0.4587 (4)	−0.6503 (5)	0.62425 (27)
C(a5)	0.5961 (4)	0.0541 (4)	0.65936 (18)	C(24)	0.4879 (4)	−0.5556 (5)	0.63018 (23)
C(a6)	0.4911 (4)	−0.0294 (4)	0.67203 (17)	C(25)	−0.1497 (4)	0.6472 (4)	0.69629 (20)
C(a7)	0.4393 (4)	−0.1970 (4)	0.65682 (18)	C(26)	−0.1392 (4)	0.6488 (5)	0.73795 (22)
C(a8)	0.4788 (4)	−0.3276 (4)	0.62652 (18)	C(27)	−0.2050 (6)	0.6448 (6)	0.75764 (25)
C(a9)	−0.0209 (3)	0.8696 (4)	0.62466 (18)	C(28)	−0.2790 (6)	0.6405 (6)	0.7359 (3)
C(a10)	−0.0696 (3)	0.7481 (4)	0.65633 (18)	C(29)	−0.2914 (4)	0.6377 (6)	0.6944 (3)
C(a11)	−0.0254 (3)	0.5802 (4)	0.67625 (17)	C(30)	−0.2265 (4)	0.6415 (5)	0.67429 (22)
C(a12)	0.0804 (4)	0.4911 (4)	0.66976 (18)	C(31)	0.1846 (4)	0.3623 (4)	0.67467 (20)
C(a13)	0.1839 (3)	0.5018 (4)	0.62723 (18)	C(32)	0.1859 (4)	0.2780 (5)	0.65185 (20)
C(a14)	0.2091 (3)	0.6086 (4)	0.58038 (18)	C(33)	0.2236 (5)	0.1912 (5)	0.66893 (27)
C(a15)	0.1731 (4)	0.7810 (4)	0.56521 (18)	C(34)	0.2572 (5)	0.1910 (5)	0.7090 (3)
C(a16)	0.0877 (4)	0.8855 (4)	0.58519 (18)	C(35)	0.2538 (4)	0.2731 (6)	0.73268 (24)
C(b1)	0.6319 (4)	−0.4206 (4)	0.56501 (20)	C(36)	0.2174 (4)	0.3588 (5)	0.71526 (23)
C(b2)	0.6849 (4)	−0.3635 (4)	0.55082 (20)	C(37)	0.2661 (4)	0.6965 (4)	0.52739 (19)
C(b3)	0.7576 (4)	−0.0075 (4)	0.56195 (20)	C(38)	0.2381 (4)	0.6594 (5)	0.48964 (22)
C(b4)	0.7450 (4)	0.0645 (4)	0.58716 (21)	C(39)	0.2837 (5)	0.6613 (5)	0.45915 (21)
C(b5)	0.5580 (4)	0.1120 (4)	0.68632 (20)	C(40)	0.3592 (5)	0.6988 (5)	0.46717 (23)
C(b6)	0.4927 (4)	0.0634 (5)	0.69296 (20)	C(41)	0.3895 (4)	0.7353 (5)	0.50437 (24)
C(b7)	0.3843 (4)	−0.2755 (5)	0.66016 (20)	C(42)	0.3431 (4)	0.7354 (5)	0.53482 (20)
C(b8)	0.4089 (4)	−0.3554 (4)	0.64206 (20)	C(43)	0.0015 (4)	1.0301 (4)	0.59443 (21)
C(b9)	−0.0889 (4)	0.9074 (5)	0.63943 (21)	C(44)	−0.0365 (4)	1.0599 (4)	0.55690 (22)
C(b10)	−0.1192 (4)	0.8326 (5)	0.65855 (20)	C(45)	−0.0648 (4)	1.1566 (5)	0.55076 (26)
C(b11)	−0.0296 (4)	0.4895 (5)	0.69808 (19)	C(46)	−0.0528 (5)	1.2226 (5)	0.5820 (3)
C(b12)	0.0353 (4)	0.4357 (4)	0.69438 (18)	C(47)	−0.0129 (5)	1.1951 (5)	0.6190 (3)
C(b13)	0.2458 (4)	0.4615 (4)	0.60775 (22)	C(48)	0.0143 (4)	1.0980 (5)	0.62556 (23)
C(b14)	0.2593 (4)	0.5240 (4)	0.57843 (21)	C(49)	0.0373 (6)	−0.0050 (8)	−0.2530 (4)
C(b15)	0.1864 (4)	0.8766 (4)	0.54893 (20)	C(50)	0.0760 (7)	0.0849 (9)	−0.2571 (3)
C(b16)	0.1353 (4)	0.9389 (4)	0.56169 (21)	C(51)	0.0401 (6)	0.1716 (8)	−0.2529 (4)
C(m1)	0.7158 (3)	−0.1840 (4)	0.55389 (17)	C(52)	0.4610 (13)	0.3489 (15)	−0.2598 (6)
C(m2)	0.6603 (3)	0.0836 (4)	0.64137 (18)	C(53)	0.4235 (22)	0.4377 (28)	−0.2664 (11)
C(m3)	0.4352 (4)	−0.1037 (4)	0.67331 (17)	C(54)	0.4606 (19)	0.5392 (20)	−0.2584 (8)
C(m4)	0.5204 (3)	−0.3902 (4)	0.60438 (18)	C(55)	0.5000	0.3228 (28)	−0.2500
C(m5)	−0.0796 (3)	0.6572 (4)	0.67526 (17)	C(56)	0.4297 (19)	0.3864 (24)	−0.2744 (10)
C(m6)	0.1477 (3)	0.4559 (4)	0.65642 (17)	C(57)	0.4416 (21)	0.4844 (26)	−0.2676 (9)
C(m7)	0.2141 (3)	0.6952 (4)	0.55930 (17)	C(58)	0.5000	0.518 (4)	−0.2500

[a] The estimated standard deviations of the least significant digits are given in parentheses.

in SO_2 and the solubility is increased. However, it is to be noted that the electronic spectrum of Fe^{II}TPP in such solvents is unperturbed by the addition of SO_2. While this work was being completed, Nakamoto[15] reported the infrared spectrum resulting from the cocondensation of Fe^{II}TPP and SO_2 in an argon matrix at 20 K; they provide evidence for weak coordination of SO_2. Wayland and Mohajer[16] have reported the formation of an SO_2 adduct of Co^{II}TPP.

Our interest was primarily in the isolation of new complexes. SO_2 complexes are unlikely to be robust, and thus gentle procedures for attempting their isolation are required. It was this concern that led us to attempt to crystallize SO_2 adducts by addition of nonsolvents to the reaction system. The apparent solubilities required the use of relatively long crystallization times. The direct reaction of Fe^{II}TPP solutions with gaseous SO_2, followed by the addition of a nonsolvent, was the first reaction attempted. Several products were observed from these reactions. These are [Fe(TPP)]$_2$SO$_4$ (μ-sulfato), [Fe(TPP)(OSO$_3$H)], and a partially characterized product we denote as SO_2-I. One product, crystalline [Fe(TPP)(OSO$_3$H)], was obtained only once; all other species were isolated several times. No degradation of the porphyrin ligand was observed. In all of the above reactions, SO_2 was present in large excess. Reactions of Fe^{II}TPP with slight stoichiometric excesses of SO_2 (toluene solution) yielded either

(15) Kuroi, T.; Nakamoto, K. *J. Mol. Struct.* **1986**, *146*, 111–121.
(16) Wayland, B. B.; Mohajer, D. *J. Chem. Soc., Chem. Commun.* **1972**, 776–777.

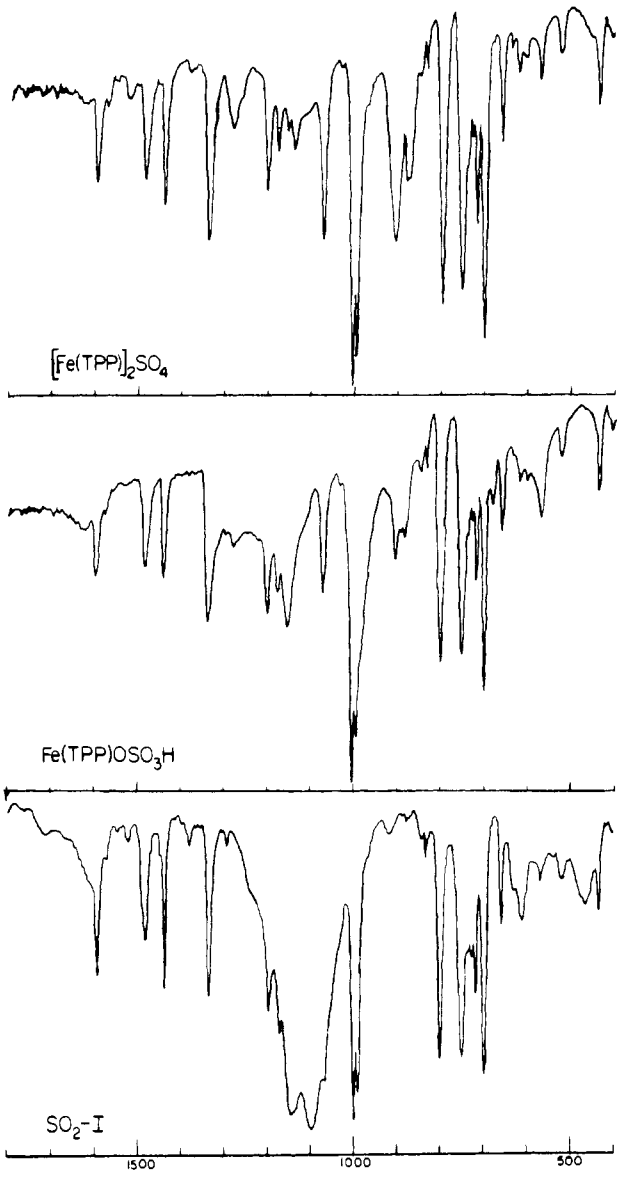

Figure 1. Infrared spectra of $[Fe(TPP)]_2SO_4$, $[Fe(TPP)(OSO_3H)]$, and SO_2-I.

starting material or the μ-sulfato complex. Reactions of $Fe^{II}TPP$ were also performed in liquid SO_2 at −40 °C. Short reaction times yield starting material upon evaporation of the SO_2, while long (>12 h) reaction times give solids with spectral properties characteristic of iron(III) porphyrinates. At no time was a μ-oxo iron(III) complex, $[Fe(TPP)]_2O$, observed in any of the reactions.

The $[Fe(TPP)]_2SO_4$ prepared above was identified by infrared and UV–vis spectral comparisons with known samples.[17,18] $[Fe(TPP)(OSO_3H)]$ was identified and characterized by a single-crystal X-ray study (vide infra) as well as by its IR spectrum. Differences in the IR spectra of $[Fe(TPP)]_2SO_4$ and $[Fe(TPP)(OSO_3H)]$ are illustrated in Figure 1. $[Fe(TPP)(OSO_3H)]$ also exhibits a typical high-spin axial EPR signal in the solid state, while $[Fe(TPP)]_2SO_4$ is EPR inactive.[17] The crystalline sample of $[Fe(TPP)(OSO_3H)]$ was obtained directly from the reaction mixture and appears unstable with respect to formation of $[Fe(TPP)]_2SO_4$. Thus, redissolution of the $[Fe(TPP)(OSO_3H)]$ obtained gave only $[Fe(TPP)]_2SO_4$ as product. However, $[Fe(TPP)]_2SO_4$ reacts with excess H_2SO_4 but does not cleanly yield $[Fe(TPP)(OSO_3H)]$. The species SO_2-I was never obtained pure

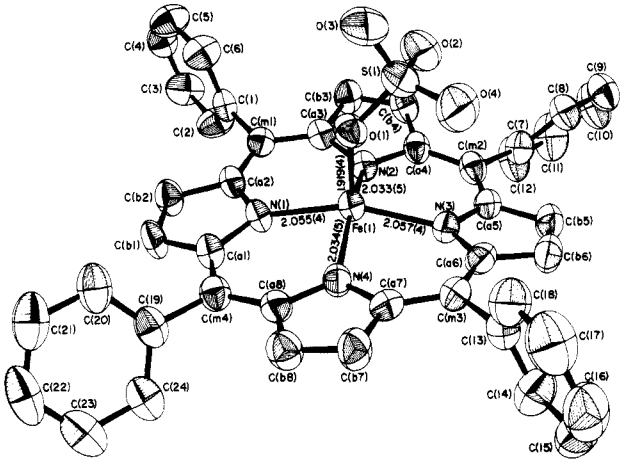

Figure 2. ORTEP diagram of the molecular structure of molecule 1 of $[Fe(TPP)(OSO_3H)]$. All thermal ellipsoids are contoured at the 50% probability level. The atom-labeling scheme and bond distances in the coordination group of the molecule are shown.

but was always contaminated with $[Fe(TPP)]_2SO_4$. All attempts to purify this material led to complete conversion to $[Fe(TPP)]_2SO_4$. SO_2-I has two strong absorptions in the IR spectrum at 1147 and 1098 cm^{-1} and weaker absorbances at 610 and 464 cm^{-1}, in addition to the usual porphyrin bands (see Figure 1). A reasonable suggestion for the identity would be a monomeric iron(III) porphyrinate with a unidentate, coordinated sulfate ion. The required counterion remains unidentified (but see below). The splitting of the free sulfate bands at 1104 cm^{-1} and the appearance of the 464-cm^{-1} band are consistent with this proposed structure.

A striking feature of all reaction products described above is the appearance of species containing sulfate and an oxidized metal ion. The presence of such species requires an oxidant; the two most likely are molecular oxygen and excess SO_2.[19] SO_2 as an oxidant can be ruled out on the basis that no reduced sulfur species have been observed and the fact that oxidized sulfato complexes are still observed when stoichiometric ratios of Fe/SO_2 are reacted. O_2 can be present only as a result of leakage into the reaction system, despite precautions taken to prevent it. Reactions of coordinated SO_2 with O_2 to yield sulfate complexes are known.[20] In addition, Miksztal and Valentine[21] have reported the reaction of three different peroxo metalloporphyrin derivatives with SO_2. In the reaction most pertinent to our work, reaction of $[Fe(TPP)]_2O_2$ with SO_2 leads to the production of $[Fe(TPP)]_2SO_4$. In our reactions that gave $[Fe(TPP)]_2SO_4$, SO_2 was generally in excess and it is tempting to conclude that an iron porphyrin–SO_2 complex is the reacting species. In any event, it is clear that the sensitivity of $Fe^{II}TPP$ to oxidation is substantially increased by the presence of SO_2. In our hands, the oxidation of $Fe^{II}TPP$ is not observed under similar conditions in the absence of SO_2. Finally, it should be noted that the deliberate addition of small amounts of air to the reaction systems leads solely to the preparation of $[Fe(TPP)]_2SO_4$.

The preparation of the hydrogen sulfate and SO_2-I complexes requires a reagent or reagents in addition to the oxidant. The

(17) Phillipi, M. A.; Baenzinger, N.; Goff, H. M. *Inorg. Chem.* **1981**, *20*, 3904–3911.
(18) Scheidt, W. R.; Lee, Y. J. Bartzcak, T.; Hatano, K. *Inorg. Chem.* **1984**, *23*, 2252–2254.
(19) A third possibility for the oxidant is SO_3. We consider this unlikely since the impurity level of SO_3 appears to be lower than that required for the reactions. Moreover, SO_3 appears to be rather strongly absorbed, at least compared to SO_2, on the P_4O_{10} (Aquasorb, Mallinckrodt), and thus the drying procedure will decrease the already quite low level of SO_3.
(20) Ryan, R. R.; Kubas, G. J. *Inorg. Chem.* **1978**, *17*, 637–646. Kubas, G. J. *Ibid.* **1979**, *18*, 182–188. Moody, D. C.; Ryan, R. R. *Ibid.* **1977**, *16*, 2473–2478. Horn, R. W.; Weissberger, E.; Collman, J. P. *Ibid.* **1970**, *9*, 2367–2371. Valentine, J.; Valentine, D., Jr.; Collman, J. P. *Ibid.* **1971**, *10*, 219–225. Wenschuh, E.; Hoffman, T.; Hundtke, K. *Z. Chem.* **1986**, *28*, 212–213. Cook, C. D.; Jauhal, G. S.; *J. Am. Chem. Soc.* **1967**, *89*, 3066–3067. Zdunneck, D.; Hausler, A.; Wenschuh, *Z. Chem.* **1986**, *28*, 302–308. Ritchey, J. M.; Moody, D. C.; Ryan, R. R. *Inorg. Chem.* **1983**, *22*, 2276–2280. Levison, T. J.; Robinson, S. D. *J. Chem. Soc., Dalton Trans.* **1972**, 2013–2017.
(21) Miksztal, A. R.; Valentine, J. S. *Inorg. Chem.* **1984**, *23*, 3548–3552.

Table III. Selected Bond Distances and Angles in [Fe(TPP)(OSO$_3$H)]

	A. Distances (Å)		
Fe(1)–N(1)	2.055 (4)	Fe(2)–N(5)	2.043 (4)
Fe(1)–N(2)	2.033 (5)	Fe(2)–N(6)	2.040 (4)
Fe(1)–N(3)	2.057 (4)	Fe(2)–N(7)	2.029 (4)
Fe(1)–N(4)	2.034 (5)	Fe(2)–N(8)	2.048 (4)
Fe(1)–O(1)	1.919 (4)	Fe(2)–O(5)	1.934 (4)
S(1)–O(2)	1.521 (5)	S(2)–O(7)	1.514 (5)
S(1)–O(1)	1.492 (4)	S(2)–O(5)	1.493 (4)
S(1)–O(3)	1.471 (5)	S(2)–O(6)	1.461 (5)
S(1)–O(4)	1.422 (5)	S(2)–O(8)	1.422 (5)
	B. Angles (deg)		
N(1)Fe(1)N(2)	88.02 (18)	N(5)Fe(2)N(6)	87.42 (18)
N(1)Fe(1)N(3)	156.60 (19)	N(5)Fe(2)N(7)	156.71 (19)
N(1)Fe(1)N(4)	86.58 (18)	N(5)Fe(2)N(8)	87.01 (18)
N(1)Fe(1)O(1)	102.66 (18)	N(5)Fe(2)O(5)	103.54 (18)
N(2)Fe(1)N(3)	87.70 (18)	N(6)Fe(2)N(7)	87.63 (18)
N(2)Fe(1)N(4)	157.93 (19)	N(6)Fe(2)N(8)	155.56 (19)
N(2)Fe(1)O(1)	102.36 (18)	N(6)Fe(2)O(5)	103.04 (18)
N(3)Fe(1)N(4)	88.81 (18)	N(7)Fe(2)N(8)	88.14 (18)
N(3)Fe(1)O(1)	100.73 (17)	N(7)Fe(2)O(5)	99.75 (18)
N(4)Fe(1)O(1)	99.70 (18)	N(8)Fe(2)O(5)	101.39 (18)
Fe(1)O(1)S(1)	135.27 (25)	Fe(2)O(5)S(2)	134.80 (25)
O(1)S(1)O(2)	105.84 (28)	O(5)S(2)O(6)	107.26 (27)
O(1)S(1)O(3)	106.61 (27)	O(5)S(2)O(7)	106.92 (28)
O(1)S(1)O(4)	112.2 (3)	O(5)S(2)O(8)	111.7 (3)
O(2)S(1)O(3)	109.4 (3)	O(6)S(2)O(7)	107.9 (3)
O(2)S(1)O(4)	109.2 (3)	O(6)S(2)O(8)	114.2 (4)
O(3)S(1)O(4)	113.3 (3)	O(7)S(2)O(8)	108.4 (4)

simplest set of conditions we envision is the additional presence of protons or acid and most probably results from small amounts of water.

The complete nonappearance of [Fe(TPP)]$_2$O suggested the possibility that SO_2 inserts into the Fe–O–Fe bond to yield the products described above. This possibility was tested by reacting [Fe(TPP)]$_2$O with SO_2. No reaction was observed except for long-term reactions wth multihundredfold excesses of SO_2, which gave *partial* conversion to [Fe(TPP)]$_2$SO$_4$. This suggested the possibility that the conversion was the result of low levels of SO_3, present either as an impurity in the SO_2 or as a result of oxidation of SO_2. This possibility was checked by reaction of [Fe(TPP)]$_2$O with SO_3; complete conversion of [Fe(TPP)]$_2$O to [Fe(TPP)]$_2$SO$_4$ was observed. No reaction of SO_2 was observed with other iron(III) porphyrinates.

[Fe(TPP)(OSO$_3$H)] was convincingly identified by a crystal structure determination. The molecular structure of one of the two crystallographically independent molecules of [Fe(TPP)(OSO$_3$H)] is illustrated in Figure 2. Shown in the figure is the atom-labeling scheme and bond distances in the coordination group. The other independent molecule is effectively the same and a view of it is given as a supplementary figure. As can be clearly seen, the HSO_4^- ion coordinates in a unidentate fashion to the iron(III) center to form a five-coordinate high-spin complex. Bidentate coordination, similar to that observed[17] for the nitrato complex, might have been found. To our knowledge, no structure of a monomeric bisulfate complex has been previously reported.

Table III presents values of selected bond distances and angles in the two molecules. Complete tables of individual distances and angles in the two molecules are available as Tables SIII and SIV (supplementary material). Figure 3 presents averaged values for bond parameters in the two porphinato cores. The agreement between the two molecules is evident. Figure 3 also displays the value of the atomic displacements, in units of 0.01 Å, from the mean plane of the 24-atom cores. The conformation of the porphinato core in both molecules is that of a modest S_4 ruffling. The average value of the displacement of the iron atom, 0.42 Å, and the avereage Fe–N distance of 2.042 (10) Å are both at the lower end of the range of values observed for high-spin iron(III) porphyrinates.[22] All other values involving the porphyrins appear

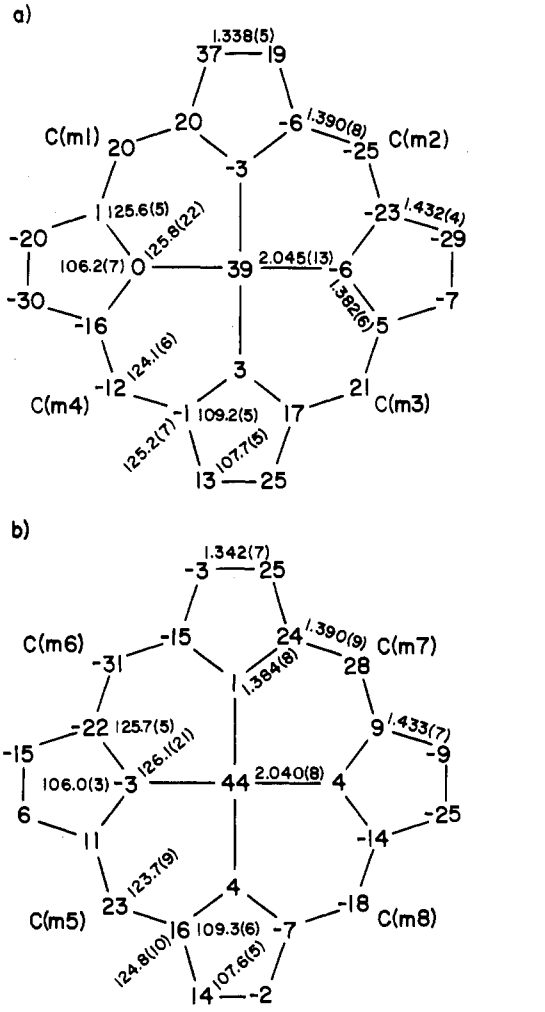

Figure 3. Formal diagrams of the porphinato cores of the molecules of [Fe(TPP)(OSO$_3$H)]·$^1/_2$C$_6$H$_6$, illustrating the displacements, in units of 0.01 Å, of each atom from the mean plane of the 24-atom core. Averaged values of bond distance and angles in each core are also displayed. Both molecules are depicted: (a) molecule 1; (b) molecule 2.

normal. The average axial Fe–O bond distance is 1.926 (11) Å. This distance is somewhat longer than that observed for high-spin iron(III) porphyrinates coordinated to phenoxide[23] (1.847 (2) Å), methoxide[24] (1.842 (4) and 1.816 (2) Å), and acetate[25] (1.898 (4) Å) and is comparable to the Fe–O bond lengths in a sulfinato complex[26] (1.92 (1) Å) and a methanesulfonato species[27] (1.94 (1) Å). The Fe–O distance in [Fe(TPP)]$_2$SO$_4$[18] is comparable but probably slightly shorter (1.894 (4) Å).

Interestingly, the HSO_4^- ion in both independent molecules is hydrogen-bonded to an adjacent HSO_4^- ion; the symmetry element relating the two ions (in each pair) is an inversion center. The structure of one of the two crystallographically unique hydrogen-bonded pairs of molecules is illustrated in Figure 4. In the two pairs, the O–H···O distances are 1.84 or 1.78 Å, while the O···O distances are both 2.63 Å. It is perhaps these hydrogen-bonding interactions that lead to the rotational orientation of the HSO_4^- ion. The dihedral angle formed by the Fe–O–S plane and an N–Fe–O plane is 22° (25°). The equivalent angles in a number

(22) Scheidt, W. R.; Reed, C. A. *Chem. Rev.* **1981**, *81*, 543–555.

(23) Goff, H. M.; Shimomura, E. T.; Lee, Y. J.; Scheidt, W. R. *Inorg. Chem.* **1984**, *23*, 315–321.

(24) Hoard, J. L.; Hamor, M. J.; Hamor, T. A.; Caughey, W. S. *J. Am. Chem. Soc.* **1965**, *87*, 2312–2319. Lecomte, C.; Chadwick, D. L.; Coppens, P.; Stevens, E. D. *Inorg. Chem.* **1983**, *22*, 2982–2992.

(25) Oumous, H.; LeComte, C.; Protas, J.; Cocolios, P.; Guilard, R. *Polyhedron* **1984**, *3*, 651–659.

(26) Cocolios, P.; Lagrange, G.; Guilard, R.; Oumous, H.; LeComte, C. *J. Chem. Soc., Dalton Trans.* **1984**, 567–574.

(27) Li, N.; Levendis, D.; Coppens, P.; Kastner, M. E.; Carruth, L. E.; Scheidt, W. R. *Acta Crystallogr., Sect. C* **1987**, *C43*, 1835–1838.

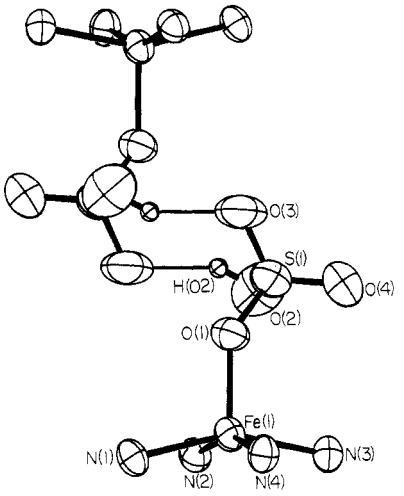

Figure 4. ORTEP diagram illustrating the hydrogen-bond arrangement between an inversion-related pair of [Fe(TPP)(OSO_3H)] molecules.

of perchlorate metalloporphyrin derivatives,[28] another group of oxyanion-ligated species, are all close to 0°, an orientation that minimizes the nonbonded interactions between porphinato core atoms and the oxygens. In [Fe(TPP)(OSO_3H)], these interactions are minimized by an increased value for the Fe–O–S bond angle (135.0°), an increase of 5–10° over the analogous angle in the various perchlorates.

The unidentate HSO_4^- ion in both molecules has the same interesting pattern in its S–O distances. Each S–O distance in the ion appears to be different from the others. As might be expected, the longest S–O distance in each ion involves the oxygen atom bonded to the hydrogen atom of the HSO_4^- ion; the next longest involves the oxygen atom coordinated to the iron(III) porphyrinate. The oxygen atom that is the hydrogen-bond acceptor is next longest, while the shortest distance involves the oxygen atom that is simply bonding to sulfur. For the reader's convenience, the S–O distances of Table III are organized in the order of the above interactions; the strong similarity in values between the two molecules is evident.

The hydrogen bonding between pairs of molecules in [Fe(TPP)(OSO_3H)] and the resultant effect that leads to the various types of S–O bonds (Table III) suggest that there should be equivalent effects on the HSO_4^- vibrational spectra. It is thus reasonable to suggest that the identity of the SO_2-I species is a non-hydrogen-bonded solid-state form of [Fe(TPP)(OSO_3H)]. It further seems plausible that the observed hydrogen-bond interactions serve to stabilize the anion in its bisulfate form and retard the conversion of [Fe(TPP)(OSO_3H)] to $[Fe(TPP)]_2SO_4$.

Acknowledgment. We thank the National Institutes of Health (Grant GM-38401-16) for support.

Supplementary Material Available: Figure S1, showing an ORTEP diagram of molecule 2, and Tables SI–SV, listing complete crystal data and intensity collection parameters, anisotropic temperature factors for all atoms, fixed hydrogen atom coordinates, and complete tables of bond distances and angles in the two molecules (13 pages); a table of observed and calculated structure factors (×10) (20 pages). Ordering information is given on any current masthead page.

(28) (a) Spaulding, L. D.; Eller, P. G.; Bertrand, J. A.; Felton, R. H. *J. Am. Soc.* **1974**, *96*, 982–987. (b) Song, H.; Rath, N.; Reed, C. A.; Scheidt, W. R. To be submitted for publication. (c) Barkigia, K. M.; Spaulding, L. D.; Fajer, J. *Inorg. Chem.* **1983**, *22*, 349–351. (d) Reed, C. A.; Mashiko, T.; Bentley, S. P.; Kastner, M. E.; Scheidt, W. R.; Spartalian, K.; Lang, G. *J. Am. Chem. Soc.* **1979**, *101*, 2948–2958. (e) Masuda, H.; Taga, T.; Osaki, K.; Sugimoto, H.; Yoshida, Z.-I.; Ogoshi, H. *Inorg. Chem.* **1980**, *19*, 950–955. (f) Gans, P.; Buisson, G.; Duee, E.; Marchon, J.-C.; Erler, B. S.; Scholz, W. F.; Reed, C. A. *J. Am. Chem. Soc.* **1986**, *108*, 1223–1234.

Contribution from the NMR Section, Department of Radiology, Massachusetts General Hospital and Harvard Medical School, Boston, Massachusetts 02114

Solution Structure and Dynamics of Lanthanide(III) Complexes of Diethylenetriaminepentaacetate: A Two-Dimensional NMR Analysis

Bruce G. Jenkins and Randall B. Lauffer*

Received June 27, 1988

The solution structure and dynamics of lanthanide(III) complexes of diethylenetriaminepentaacetate (DTPA) have been investigated by ^1H NMR. Two-dimensional (2D) exchange spectroscopy (EXSY) enables the determination of solution dynamics. At low temperatures (0–25 °C) the complexes $Pr(DTPA)^{2-}$, $Eu(DTPA)^{2-}$, and $Yb(DTPA)^{2-}$ are in slow exchange on the NMR time scale, and all 18 proton chemical shifts are resolved. Raising the temperature causes the number of resonances to decrease from 18 to 9, consistent with exchange between two enantiomers. The rates of exchange of the complexes follow the order Pr(III) < Eu(III) < Yb(III). Utilization of 2D correlation spectroscopy (COSY) along with EXSY data as constraints enables assignments of the chemical shifts via calculations of the dipolar shifts. These calculations afford many reasonable solutions with low *R* factors, and only through the use of the 2D COSY and EXSY data can certain solutions be rejected. These calculations also confirm that the previously published crystal structure of $Nd(DTPA)^{2-}$ can quite satisfactorily explain the solution structure. In addition, these data indicate that the central acetate moiety is coordinated to the metal in solution.

Introduction

The solution structure and dynamics of multidentate lanthanide(III) complexes are not well understood. These complexes generally have coordination numbers of 8–10 with greatly varying coordination polyhedra.[1,2] Questions that arise include the following: (i) Are the solution structures the same as that in the solid state? (ii) Can the total coordination number vary as a function of temperature or across the lanthanide series? (iii) What factors control the intramolecular dynamics?

The importance of these issues has been enhanced by the recent development of gadolinium(III) complexes as diagnostic pharmaceuticals for clinical ^1H NMR imaging.[3] These agents are injected intraveneously to alter the water proton relaxation times of tissues and improve image contrast and information content. The prototype agent, aquogadolinium(III) diethylenetriaminepentaacetate [$Gd(DTPA)(H_2O)^{2-}$], has undergone extensive clinical trials[4] and is now approved for human use in the U.S. It

(1) Williams, R. J. P. *Struct. Bonding* **1982**, *50*, 79.
(2) Sinha, S. P. *Struct. Bonding* **1976**, *45*, 69.
(3) Lauffer, R. B. *Chem. Rev.* **1987**, *87*, 901.

0020-1669/88/1327-4730$01.50/0